Structural, Optical and Electrical Properties of Y_2O_3 in Borosilicate Glasses

Thesis submitted in partial fulfilment of requirement for the award of degree of

MASTER OF TECHNOLOGY

IN

MATERIAL SCIENCE AND METALLURGY

Submitted by:

GAURAV KALIA

Reg. No. 601202005

Under the supervision of:

Dr. KULVIR SINGH

PROFFESSOR & HEAD

SCHOOL OF PHYSICS AND MATERIAL SCIENCE

THAPAR UNIVERSITY

PATIALA-147004

JULY-2014

CERTIFICATE

I, hereby, certify that the Thesis entitled **"Structural, Optical and Electrical properties of Y_2O_3 in borosilicate glasses"** submitted in the partial fulfilment of the requirement for the degree of Master of Engineering in Material Science and Metallurgy, in the department of School of Physics and Material Science , Thapar University, Patiala is an authentic work carried out by me under the guidance of **Dr. Kulvir Singh**, Professor and Head , Thapar University and refers other researcher's works, which are duly listed in the reference section. To the best of my knowledge, the matter embodied in the thesis has not been submitted to any other university/institute for the award of any degree or diploma.

This is certifying that the above statement made by the student is correct and true to the best of my knowledge and belief.

(Dr. Kulvir Singh)
Professor and Head
Thapar University

Countersigned by:

(Dr. Kulvir Singh)
Professor and Head, SPMS
Thapar University

(Dr. S.K. Mohapatra)
Dean (academic affairs)
Thapar University

Dedicated to my parents

DECLARATION

I hereby declare that the work being presented in this thesis report entitled **"Structural, Optical and Electrical Properties of Y_2O_3 in Borosilicate Glasses "** by me in partial fulfillment of the requirements of the award of degree of **Master of Technology** in **Materials Science and Engineering** from **School of Physics and Materials Science**, Thapar University, Patiala is an authentic record of my work carried out under the supervision of **Dr. Kulvir Singh, Professor and Head, School of Physics and Materials Science, Thapar University**. The matter presented in this report has not been submitted in any other University/Institute for the award of Masters of Technology or any other degree.

Gaurav Kalia

Reg. No. 601202005

ACKNOWLEDGEMENT

I am highly grateful to authorities of Thapar University, Patiala for providing this opportunity to carry out the thesis work. To begin with, I would like to express my sincere gratitude to my Supervisor Dr. Kulvir Singh, *Professor and Head of School of Physics and Materials Science, Thapar University, Patiala* for his steady and continuous guidance throughout my entire candidature. I would like to express my heartfelt gratitude to him for introducing me to my current research area and also, guiding and supporting me throughout my research work.

I thank Dr. B. N. Chudasama, *Assistant Professor and in-charge, Sophisticated Lab, School of Physics and Materials Science, Thapar University, Patiala* for the access to UV-Vis spectrophotometer for sample characterization during my research. Also, I thank Mr. M. Aggarwal and Mr. Ghanshyam Maurya of *Sophisticated Analytical Instrumentation Laboratory, Thapar University, Patiala* for their help.

I am very grateful to Mr. Satwinder Singh (Research Scholar) for his outmost help through valuable guidance during experiment. I would also like to express my sincere gratitude to Ms. Samita Thakur, Pooja Singla and Ms. Sakshi Gupta for making me part of healthy discussions and for helping me with my doubts. I also thank Mr. Gaurav Singla, Mr. Paramjyot Jha, Ms. Chandani Khurana, Ms. Parveer Kaur, Ms. Purnima Sharma, Ms. Gitanjali Dhir and Mr. Jaspal Singh for their timely helps. I wish to sincerely thank our lab technicians Mr. Jant Singh and Mr. Purshotam Singh.

I wish to express my deep gratitude to my family and my friends (Bharat, Pritampal, Hitesh, Deepshikha, Amit, Gaganjot, Kripal, Mahesh) for their whole-hearted and unconditional support throughout my research.

Finally, I would like to acknowledge the financial support provided by School of Physics and Materials science, Thapar University, Patiala, and Ministry of Human Resource Development (TEQIP scheme) in the form of research grant and teaching assistant scholarship.

ABSTRACT

Glass and glass ceramic samples with composition $55SiO_2$-$30B_2O_3$-xLi_2O-$(15-x)Y_2O_3$, where x=0, 5, 10, 15 have been prepared by melting and quenching technique. The structural and optical properties of these samples have been studied using various techniques like X-ray diffraction (XRD), Fourier Transform Infra Red spectroscopy (FTIR), UV-visible spectroscopy and impedance spectroscopy. Samples for x = 5 and 10 are purely amorphous in nature as indicated by XRD patterns of these samples. On the other hand, samples for x=0 and 15 show some degree of crystallinity. A broad halo was observed in all the samples, which originates from their amorphous part. Optical band gap of the samples decreases with increasing Y_2O_3. Urbach energy decreased with increase in Li_2O. The effect of temperature on the conductivity of the sample YL-5 was observed. It was found that the conductivity increased with the increase in temperature. The conductivity of YL-5 sample was found to be ~$5*10^{-6}$ s/cm at 600^oC.

LIST OF ABBREVIATIONS

BJT	-	Bipolar Junction Transistor
MOSFET	-	Metal Oxide Semiconductor Field Effect Transistor
XRD	-	X-Ray Diffraction
FTIR	-	Fourier Transform Infrared Radiation
UV-visible	-	Ultra violet visible spectroscopy
NBOs	-	Non-Bridging Oxygen

LIST OF FIGURES

Contents

Chapter 1 Introduction

1.1 **Background**

The history of glassmaking can be traced back to 3500 BC in mesopotamia. Archaeological evidence suggests that the first glass was made in coastal north Syria, mesopotamia or Ancient Egypt [1]. The earliest known glass objects, of the mid third millennium BC, were beads, perhaps initially created as accidental by-products of metal-working (slags) or during the production of faience, a pre-glass vitreous material made by a process similar to glazing [2].

The development of glass technology in South Asia may have begun in 1730 BC [3]. In ancient China, though, glassmaking seems to have a late start, compared to ceramics and metal work. In the Roman Empire, glass objects have been recovered across the Roman Empire in domestic, industrial and funerary contexts. Anglo-Saxon glass has been found across England during archaeological excavations of both settlement and cemetery sites. Glass in the Anglo-Saxon period was used in the manufacture of a range of objects including vessels, beads, windows and jewelry.

The earliest development in glass making and its proper documentation description was given by moody et al. [4]. Earlier times glasses were formed using sand and an alkali flux obtained from plant ash. By mediaeval times it was known that leaching the ash and purifying the alkali by evaporation leads easy melting of the glass. Unfortunately this process of glass making show serious problem of chemical durability [5].

Enormous advances were made in glass technology during the last century. The title of most eminent glass technologist of all time should probably be awarded to Joseph Fraunhofer [6]. The glass produced to make good achromatic doublets. Fraunhofer's have developed a mechanism to develop a mechanism to test the durability of glasses. Although, chemistry was advancing rapidly, Fraunhofer would have been hindered by lack of pure materials and inability to analyze them or his glasses. These problems were rather less severe for Michael Faraday, the most creative of all scientists to have spent some of his time working as glass

technologist, who had better resources close to hand. In twentieth century the possibility of solids reacting together was becoming widely recognized and some of the earliest systems studied were of interest to glass makers. During world war-II, the British glass industry was suffered because it was totally dependent on Germany. Therefore et al [7] formed glass society a department related to glass technology in Sheffield university U.K. The first successful attempt to produce an approximate theory to describe the kinetics of solid state reactions was by Jander (1927) who used data for systems including carbonates and silica to support his theory. This developed an interest in studies of glass making reactions among chemists as well as glass technologists [5].

The last two decades have seen the need for glasses with much smaller transmission losses than previously imagined to be feasible, for use in optical communication systems and this has been the application of glass encouraged the research in the field of glasses. This has also led to the development of halide glasses made in systems never before considered capable of producing glasses or worth investigation. Subsequently the developments have led to studies of other possible optical communication devices including optical switches and amplifiers; this has encouraged detailed studies of glasses with nonlinear optical properties. Glasses are usually good electrical insulators but can be made with a very wide range of electrical properties including semi-conduction and fast ion conduction. In addition to so many applications of glasses, recently, glasses are also being used as a sealant the energy technology [5].

1.2 Glasses

Glass is an amorphous (non-crystalline) solid material that exhibits a glass transition, which is the reversible transition in amorphous materials from a hard and relatively brittle state into a molten or rubber-like state. Glasses are typically brittle and may or may not be optically transparent. The most familiar type of glass is soda-lime glass, which is composed of about 75% silicon dioxide (SiO_2), sodium oxide (Na_2O) from soda ash, lime (CaO), and several minor additives. The glasses are familiar group of ceramics; container, lenses, and fiber glass represent typical application. As above mentioned they are non-crystalline silicates containing oxides, mainly CaO, Na_2O, K_2O and Al_2O_3 which influence the glass properties.

Silicate glass generally has the property of being transparent. Because of this, it has a great many applications. One of its primary uses is as a building material, as small panes set into window openings in walls. Additionally, in its most solid forms, it has also been used for paperweights, marbles, and beads. Glass is both reflective and refractive of light, therefore these materials can be used for optical lenses, prisms and fine glassware. Colored glasses can be obtained by addition of transition element in glass composition [7]. These qualities have led to the extensive use of glass in the manufacturing of art objects. Although brittle, glass is extremely durable, and many examples of glass fragments exist from early glass-making cultures.

1.3 Structure of glass

The structure of liquids, glasses and other amorphous solids is characterized by the absence of long-range order, which defines crystalline materials. Liquids and amorphous solids possess a rich and varied array of short to medium range order, which originates from chemical bonding and related interactions. Metallic glasses, for example, are typically well described by the dense random packing of hard spheres, whereas covalent systems, such as silicate glasses, have sparsely packed, strongly bound, tetrahedral network structures. These very different structures result in materials with very different physical properties and applications.

The study of glass structure aims to gain insight into its behavior and physical properties, so that it can be understood, predicted and tailored for specific applications. Since the structure and resulting behavior of glasses is a complex many body problem, it is too computationally intensive to solve using quantum mechanics directly. Instead, a variety of diffraction, NMR, Molecular dynamics, and Monte Carlo simulation techniques are most commonly used.

Early theories relating to the structure of glass included the crystallite theory whereby glass is an aggregate of crystallites. However, structural determinations of vitreous SiO_2 and GeO_2 made by Warren and co-workers in the 1930s using x-ray diffraction showed the structure of glass to be typical of an amorphous solid. Zachariasen [8] introduced the random network theory of glass in which the nature of bonding in the glass is the same as in the crystal but where the basic structural units in a glass are connected in a random manner in contrast to the periodic arrangement in a crystalline material. Despite the lack of long range order, the

structure of glass does exhibit a high degree of ordering on short length scales due to the chemical bonding constraints in local atomic polyhedra [9]. For example, the SiO_4 tetrahedra that form the fundamental structural units in silica glass represent a high degree of order, i.e. every silicon atom is coordinated by four oxygen atoms and the nearest neighbor Si-O bond length exhibits only a narrow distribution throughout the structure. The tetrahedra in silica also form a network of ring structures, which leads to ordering on more intermediate length scales of up to approximately 10 Å.

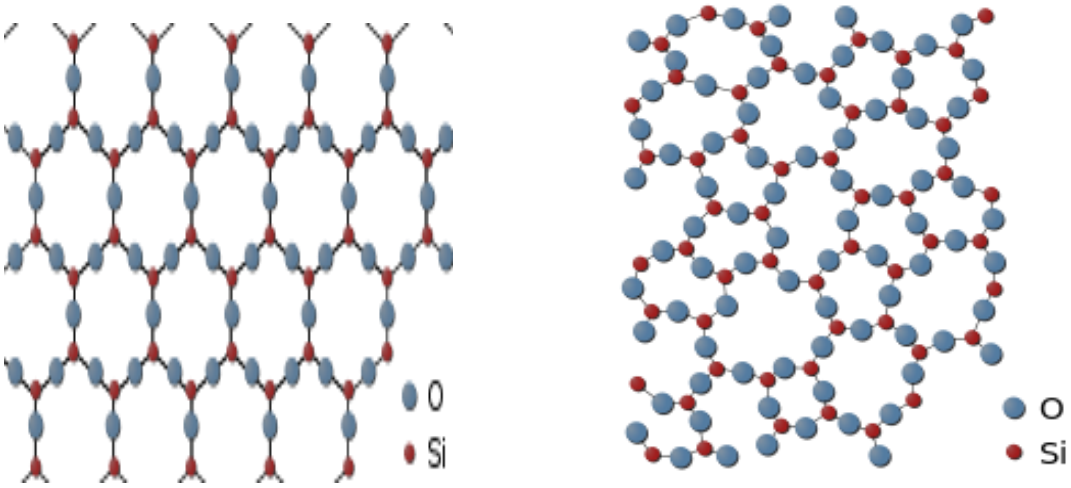

(a) (Crystalline SiO_2) **(b) (Amorphous Sillica)**

Fig. 1. 1 Structure of glass [5]

1.4 Classification of Glasses

Based on the chemical composition, a large number of glasses with different chemical and physical properties can be prepared. Glasses can be classified into following categories:

1.4.1 Silicate Glasses

Silica (SiO_2) is a common fundamental constituent of glass. In nature, verifications of quartz occurs when lightning strikes sand, forming hollow, branching root like structures called fulgurite. While fused quartz (primarily composed of SiO_2) is used for some special applications, it is not very common due to its high glass transition temperature of over 1200 °C. Normally, other substances are added to simplify processing. Such as sodium carbonate (Na_2CO_3, "soda"), which is used to lowers the glass transition temperature (T_g). However, the soda makes the glass water soluble, which is usually undesirable, so CaO, MgO, Al_2O_3 are added to provide a better chemical durability. The resulting glass contains about 70 to 74% silica by weight and is called a soda-lime glass [10].

Most common glass contains other ingredients added to change its properties. Lead glass or flint glass is more 'brilliant' because the increased refractive index causes noticeably more specular reflection and increased optical dispersion. Adding barium also increases the refractive index. Thorium oxide gives glass a high refractive index and low dispersion initially it was formerly used in producing high-quality lenses, but due to its radioactivity, it has been replaced by lanthanum oxide in modern eye glasses. Iron can be incorporated into glass to absorb infrared energy, for example, in heat absorbing filters for movie projectors, while cerium (IV) oxide can be used for glass that absorbs UV wavelengths [11]. When alkali silicate glasses are mixed with some sesquioxides (e.g., Sb_2O_3, Al_2O_3, Y_2O_3, and La_2O_3 etc.), their thermo-physical, chemical and mechanical stability will be further improved. Such glasses were proved to be high efficient luminescence materials [12-18], and may be considered as good candidates for integrated optics, photon [19-23].

1.4.2 Borate Glasses

In borate glass, melt of composition rich in B_2O_3 show high viscosity and tendency to form a glass. It allows the preparation of glasses that may possess interesting physical properties for optical application. The action of alkali ions as modifiers in borate glasses is more complex than that in silicate glasses. In the latter the addition of alkali ions leads invariably to the

creation of non-bridging oxygens (NBOs) where the NBO concentration increases linearly with the alkali content and depending on the amount of modifier.

Jan Krogh-Moe [24] contribution a lot in research of borate based glasses. Krogh-Moe proposed that borate glasses contain well defined and stable polyborate groups which also occur in borate crystals. Borate glasses present very interesting features such as optically transparency from the visible to the near-infrared range, wide compositional regions of PbO content in the host glass matrix, high refractive index and density, good transmittance in the UV-region and enhanced radiation shielding for ϒ-rays. In fact, lead borate glasses are already being used in enamels, photonics, and optoelectronic applications.

1.4.3 Phosphate Glasses

Phosphate glasses are materials based on phosphorus pentoxide (P_2O_5), usually with some added chemical components [25]. They are used as laser gain media – both in bulk lasers and in the form of optical fibers. One of their primary advantages is their very high solubility for rare earth ions such as erbium (Er^{3+}), ytterbium (Yb^{3+}) and neodymium (Nd^{3+}). This means that high concentrations of laser-active rare earth ions can be incorporated into phosphate glasses without detrimental effects such as clustering, which could degrade the performance via quenching effects. For example, erbium-doped fibers can be made with much higher doping concentrations than silica fibers: several weight percent are possible. Its application, research is limited due to its hygroscopic nature.

1.4.4 Halide glasses

Halides glasses are based entirely on heavy metal inorganic fluorides. The most studied chemical composition is $57ZrF_4$-$36BaF_2$-$4LaF_3$-$3AlF_3$ (ZBLA). In general, the typical fluoride glass has a glass transition temperature, T_g, four times less than silica, is considerably less stable, and has practical failure strains of only a few percent compared to silica's greater than 5%. While an enormous number of multicomponent fluoride glass compositions have been fabricated, comparably few have been drawn into fiber. An important feature of the fluoroaluminate glass is its higher T_g, which largely accounts for the higher laser damage

threshold for the fluoroaluminate glasses compared to ZBLAN at the Er:YAG laser wavelength of 2.94 nm.

1.4.5 Chalcogenide Glass

Chalcogenide glass is a glass containing one or more chalcogenide elements (not counting oxygen). The name chalcogenide originates from the Greek word "chalcos" meaning ore and "gen" meaning formation, thus the term chalcogenide is generally considered to mean ore former. These are three elements sulfur, selenium and tellurium. Such glasses are covalently bonded materials and may be classified as network solids; in effect, the entire glass matrix acts as an infinitely bonded molecule. Polonium is chemically a chalcogenide as well, it is not used in chalcogenide glasses because of its strong radioactivity and high cost. Oxygen also however it belongs to same group element, however it is not considered a chalcogenide. Though oxide materials are the oldest known glass forming systems it has become more traditional to treat them separately from more recently discovered chalcogenide compounds. Scientifically, oxide materials behave rather differently from other chalcogenides, in particular their widely different band gaps contribute to very dissimilar optical and electrical properties [5].

1.4.6 Metallic Glasses

Metallic glass is a solid metallic material, usually an alloy, with a disordered atomic-scale structure. Glass having metallic properties is obtained from a melt containing metallic element instead of oxide. Most metals are crystalline in their solid state, which means they have a highly ordered arrangement of atoms. Unlike common glasses, such as window-glass, which are typically insulators, amorphous metals have good electrical conductivity. There are several ways in which amorphous metals can be produced, including extremely rapid cooling, physical vapor deposition, solid-state reaction, ion irradiation, and mechanical alloying [26].

1.5 Properties of Glasses

The special properties of glasses are related to their liquid like structure. The property of transparency is character of liquid than that of solid state. Glasses are isotropic and lack

internal grain boundaries or structural elements lying in specific orientation. Some of the special properties of glasses are given below:

1.5.1 Physical Properties

Density of glass is a strong function of its composition and most important measure of glass. It also stands on its own as an intrinsic property capable of casting light on short range structure. The addition of network modifier component increases the density as network modifier ions attempt to occupy the interstices within the network. The addition of alkalis metals to silica results in an increase in density.

1.5.2 Thermal Properties

The expansion and contraction due to thermal energy is an important consideration for product design. When a glass is heated it expands. If the temperature over the body of glass is equal everywhere and body is not restrained then there will be no development of stress in the body. On the other, hand if there is non-uniform heating of body, then the different layer of glass attempt to expand differently and consequently stress develop. The magnitude of stress so generated is related to thermal expansion. Addition of modifier in glass increases the bond bending which automatically increase the thermal expansion. Thermal expansion of glasses with few exceptions increases with increase in temperature. The increase in thermal expansion arise from the increase in non-bridging oxygen concentration which increases the average asymmetry of Si-O bond and from the filling of interstices which interfere with bond bending mechanism responsible for low thermal expansion. Vitreous silica display negative thermal expansion coefficient over the temperature range 227-727^{o}C. The negative thermal expansion coefficients are believed to result from ability of network to absorb lattice expansion through bending of bonds into empty interstices of the structure. The addition of alkali increases the thermal expansion. Thermal expansion is a volume averaged function of contribution of each of the phases present in a sample, formation of crystal with the thermal expansion coefficient which are very different from initial glass can radically alter the thermal expansion coefficient of the composite. Formation of crystal can also change the value of T_g and crystallization temperature (T_c) by changing the composition of residual glass.

Commercial lithium aluminosilicate glass ceramic provide excellent examples of such behavior. The initial glass used for production of transparent cookware, for example, has a thermal expansion coefficient of $4*10^{-6\ O}C$, $T_g = 730^oC$ and $T_c = 760^oC$. After processing the thermal expansion coefficient is 0.5*10-6 $^OC\ K^{-1}$ and T_g and T_c can no longer be detected on the expansion curve below 1000^oC. Heat treatment results in the formation of lithium aluminosilicate crystal which has very low thermal expansion coefficient. Removal of lithium from the residual glassy phase also decreases the thermal expansion coefficient of that phase, while simultaneously increasing the transformation and softening temperature.

1.5.3 Optical Properties

The major technological development that have added to comfort of living are glass lenses as an aid to failing vision, glass window to bring daylight into housing structure while providing protection from harsh particle, dust particles etc. Glass in the light bulb provides light in the dark and glass fiber in enhanced communication [27]. Optical properties of glasses are subdivided into three categories first many application based on bulk optical properties such as refractive index and optical dispersion. Other property including color based on optical property which is strong function of wavelength and last is nontraditional optical effect.

1.5.3.1 Bulk optical properties:

Development of early telescope and microscope is a search of new optical glasses with appropriate refractive index and optical dispersion. Refractive index remains the most measured optical properties of glass and most basic optical property for determination of appropriate glass. The refractive index is defined as ratio of velocity of light in vacuum divided by velocity of light in medium. This ratio can be measured by Snell's law

$$n = \sin\theta_i / \sin\theta_r \qquad (1)$$

Where n= refractive index, θ_i= angle of incident and θ_r= angle of refractive

The variation in index with wavelength is called optical dispersion. Dispersion is defined by entire curve of refractive index with respect to wavelength.

1.5.3.2 Ultra violet absorption:

Even transparent colorless glasses cannot transmit radiation at wavelength beyond their inherent ultraviolet edge. This frequency is due to transition of valance electron to the excited state. Conversion of bridging state of oxygen to non-bridging state of oxygen will lower the energy required for electronic excitation and shift the ultraviolet edge to lower frequency. Addition of alkali oxides to silica result in shift of ultraviolet edge toward the visible region.

1.5.3.3 Infrared absorption:

Absorption of light in ultraviolet and visible region is due to electronic transition. While there is lower energy electronic transition in the infrared region of spectrum, most optical absorptions in this region are due to vibrational transition. These absorptions are due to impurity absorption due to gases and the fundamental structural vibration. Glasses are very interesting materials with useful properties such as:

- Glasses form the basic elements of virtually all optical systems.
- Glasses are among the few solids that transmit visible light.
- World-wide telecommunications by optical fibers.
- High refractive index.

1.5.4 Electrical Properties

Ionic conductivity in glass has been studied for over a hundred years and there are indications that glassy (and amorphous) electrolytes being used in all-solid-state batteries and in electrochromic devices. These developments are at an early stage, and much effort is still being directed toward discovering new glassy systems and to optimizing the levels of ionic conductivity in these materials. Remarkably, the main electrical application of ionic conductivity is still in the use of glass electrodes in analytical chemistry where very low levels of conductivity suffice, and the dominant effect is the surface interaction. By way of contrast, the existence of semiconducting glasses has been clearly recognized for only some twenty years ago. They find technological applications, in xerography, solar cells for pocket calculators. This difference in the pace of technological development is part of a wider

experience in the field of solid state ionics, and points up the difficulties in establishing reliable electrode-electrolyte interfaces and in avoiding unwanted chemical and electrochemical side reactions. To complicate matters further, many of the glasses which are good ionic conductors are either very hygroscopic or else sensitive to light. By contrast, materials widely used in microelectronics applications such as amorphous silicon (a-Si) are remarkably robust, and can also be used in architectural applications. Apart from these technical aspects, considerable progress has been made in recent years in understanding the mechanisms of both ion and electron transport in glasses and amorphous materials.

In the case of ionic conductivity, the focus is naturally on identifying the links between ion mobility on the one hand and glass structure and chemical bonding on the other. Some theoretical approaches, such as the weak electrolyte and ionic interaction theories, draw attention to more general solution of these phenomena.

The electrical properties (and especially the key role of dopants) are also very much influenced by chemical equilibria involving electron donors and acceptors, as well as defects in the glass structure. In effect, there is a growing tendency for theoretical discussions in the fields of ionic and electronic conductivity to converge on problems in glass chemistry. However, historically there has been some tendency for ionic and electronic processes to be treated as distinct phenomena, with chemists concentrating largely on ionic, and physicists on electronic systems.

Although most glasses contain charged metallic ions capable of carrying an electric current, the high viscosity of glass impedes their movements and electrical activity. Thus, glass is an efficient electrical insulator—though this property varies with viscosity, which in turn is a function of temperature. Indeed, the electrical conductivity of glass increases rapidly with temperature. Since univalent alkali ions have the greatest mobility through the glassy structure, they are the primary charge carriers of a glass and therefore determine its electrical conductivity. In general, the higher the concentration of alkali metals, the higher the electrical conductivity. The most noted exception, from the additivity relationship, here is the mixed-alkali effect, in which glasses containing two or more different types of alkali ions have a significantly lower electrical conductivity than linear additivity would suggest. In applications

such as high-voltage lamps, where low electrical conductivity is desired, mixed-alkali glasses are very useful [28].

1.5.5 Mechanical Properties

Glasses are brittle material as a result fracture behavior is usually determined by environmental factor and not by inherent strength of the bond forming the vitreous network [29]. The fracture strength of glasses varies with prior surface treatment, chemical environment and inherent stress etc. the glasses are also quit susceptible to failure due to thermal shock. Other mechanical properties of glasses are inherent to material. The elastic modulus is determined by individual bond in materials and by structure of network. The hardness of glass is a function of strength of individual bond and density of packing of atom in localized structure.

In the next chapter, recent development in the field of glasses, particularly optical properties are given.

Chapter 2 Literature Reviews

All over the world research is going on to search new glass materials and discover their different physical, electrical and optical properties. Recently development in the field of glass and their application particularly related to optical properties are given below.

Gedam *et al*. **[29]** prepared the glasses with composition of $25Li_2O$-$(75-x)$ B_2O_3 - xNd_2O_3 by melting quenching technique. Electrical and optical characterizations of these glasses were carried out. It was observed that conductivity of glasses decreased and activation energy increased with addition of Nd_2O_3. The density and refractive index of glasses increased while optical band gap decreased due to structural changes at the local environment.

Ahlawat *et al.* **[30]** prepared the bismuth silicate glasses containing lithium oxide with composition $20Li_2O$-$(80-x)Bi_2O_3$-$xSiO_2$ by melt quenching technique. Density and glass transition temperature have been measured. FTIR technique was used to observe the structure of these glasses in order to obtain the information about role of Bi_2O_3 and SiO_2 in the formation of glass. Increase in SiO_2 content in glass resulted in Si-O-Si bond angle, due to which ionicity increases. The value of band gap has been determined from cutoff wavelength of these glasses. It is also observed that the cutoff wavelength decreases as the content of SiO_2 increases in the glass system. The introduction of SiO_2 at the expense of Bi_2O_3 results in contraction of the glass structure and increase in glass transition temperature. From the analysis of infrared spectra of these glasses it was found that Bi^{3+} cations are incorporated in the glass network as $[BiO_6]$ octahedral units. The shifting of band around 471–456 cm^{-1} to lower wave number and of the band at 800–1180 cm^{-1} towards higher wave number suggests the increase in Si–O–Si bond angle. The presence of distorted $[BiO_6]$ octahedral units in the glass network was observed and the degree of distortion was found to be decreasing on progressive substitution of Bi_2O_3 by SiO_2.

Gedam *et al.* **[31]** synthesized a glass series with general formula $15Li_2O$–$(85-x)$ B_2O_3–$xCeO_2$ using the conventional melt quench technique. The electrical conductivity, optical properties and the coefficient of thermal expansion were measured for the prepared glasses. The conductivity of the glasses decreased with the addition of CeO_2 because the mobility of Li^+

ions and the compactness of the glass structure decreased. The density and the refractive index of the glasses increased, whereas, the optical band gap and the radiation length decreased because of the increase in density and decrease in CTE along with the average boron–boron (‹d_{B-B}›) distance with the addition of CeO_2 are complementary to each other and support the observed decrease in conductivity.

Gupta *et al.* **[32]** take the composition of SiO_2–MgO–B_2O_3–Y_2O_3–Al_2O_3 is different ratio and synthesized the glass. The crystallization kinetics of these glasses was observed using various characterization techniques such as differential thermal analysis (DTA), thermo gravimetric analysis (TGA), X-Ray diffraction (XRD) and scanning electron microscopy (SEM). There is change in crystallization behavior due to addition of Y_2O_3 instead of Al_2O_3. It also increase the transition temperature, T_g, crystallization temperature, T_c and stability of glasses The addition of Y_2O_3 completely suppresses the formation of cordierite phase in the rest of the glasses and enhances the stability of the glasses.

In order to improve the bending strength of glass ceramic thin tiles, **Liu** *et al*. **[33]** prepared SiO_2-ZnO-Na_2O-Y_2O_3 glasses. The influences of the thermal properties and thermal expansion coefficient of the glass and the sintering temperature on the structural properties of the composites were investigated by differential thermal analysis (DTA), X-Ray Diffraction (XRD), Raman and scanning electron microscopy (SEM). The bending strength of the composites was measured with an universal testing machine. Results show that the crystallization temperature of the SiO_2-ZnO-Na_2O-Y_2O_3 glass is higher than that of SiO_2-ZnO-Na_2O glass. The corresponding crystallites show more complex structure for the SiO_2-ZnO-Na_2O-Y_2O_3 glass. The crystallization temperature of SiO_2-ZnO- Na_2O-Y_2O_3 glass was higher. The crystallite structure of SiO_2-ZnO-Na_2O-Y_2O_3 glass was more complicated with ZnB_4O_7, $ZnSiO_4$, B_2O_3, Y_2O_3 and SiO_2 crystal structures in the glass.

Wang *et al***. [34]** synthesized the glass with composition $60SiO_2$ – (40-*x*)Al_2O-*x*Y_2O_3, respectively. Where *x*=10, 20, 30, 40. The thermal properties of glass with respect to stainless steel were assessed. The glass transition points fell in the range of 694^oC and 833^oC, while the glass softening points, varying from 725^oC to 885^oC, decreased linearly with the ZnO/SiO_2 ratio. The coefficient of thermal expansion varies from 7.01 to 9.30 x 10^{-6}/K. By adding Y_2O_3

having less thermal expansion A low leak rate of 0.052 sccm/cm was obtained and stayed unchanged after a duration of 500 h at 700^{o}C.

Kim *et al.* **[35]** prepared lithium ion conducting borosilicate glass by melt quenching technique from a mixture of Li_2CO_3, B_2O_3 and SiO_2 powders. The Li ion conductivity of the lithium borosilicate glasses was evaluated in terms of the SiO_2/B_2O_3 ratio. In the Li_2O-B_2O_3-SiO_2 ternary glass, the glass forming region decreases with an increasing Li_2O content. At the same Li_2O, the crystallization tendency of the glass samples increases with the SiO_2/B_2O_3 ratio, resulting in a reduced glass forming region in glass. The electrical conductivity moderately depends on the SiO_2/B_2O_3 ratio in these glasses. The conductivity of the glasses slightly increases with the SiO_2/B_2O_3 ratio. The observed phenomenon can be explained by the modification of the glass structure as a function of the SiO_2 content.

Dalvi *et al.* **[36]** studied the effect of Cu_2O substitution in 15Agl-10Cu_2O-50Ag_2O-25V_2O_5 glass matrix glassy nature of sample. Electrical conductivity of these samples found to be increasing with Cu_2O content and approaches to maximum value at room temperature. Ionic mobility measured using transient ionic current technique increased with Cu_2O content significantly. The sample was found to be predominantly ion conducting in nature. High Cu_2O content samples ($x \geq 0.3$) though exhibit nano composite nature as revealed by scanning electron microscopy, the conductivity enhancement is found to be due to compositional changes that eventually lead to rise in ionic mobility.

Garbarczyk *et al*. **[37]** prepared Novel nanomaterials based on lithium–vanadate-phosphate (LVP) and lithium–iron-phosphate (LFP) glasses. Their electrical properties were investigated by impedance spectroscopy. It was found out that the electronic conductivity of the original glasses of both systems can be considerably enhanced by appropriate annealing at temperatures close to beginning of crystallization temperatures determined by DSC/DTA methods. Increase in conductivity arises from the modification of the microstructure. It was observed that by appropriate heat-treatment glasses of both systems, they can be turned into nanomaterials consisting of crystallites smaller than 100 nm embedded in the glassy matrix. It was postulated that the major role in the conductivity enhancement of these nanomaterials is played by the developed interfacial regions between nanocrystalline and glassy phases.

Kaur *et al*. [**38**] studied the optical and structural properties of $15Bi_2O_3$-$10Al_2O_3$-$50B_2O_3$–$25SiO_2$ glasses prepared by melting followed by quenching method. Effect of heavy ion irradiation on glass network and structural units have been studied by irradiating glass thin film samples with heavy ions Li^{3+} (50 MeV) and Ag^{14+} (180MeV) at different fluence rate sranging from 10^{12} ions/cm^2 to 10^{14} ions/cm^2. Irradiation of materials by swift heavy ions (SHI) resulted in highly excited lattice atoms due to inelastic collisions with atomic electrons. Atomic displacements and structural modifications of such a lattice, brings out interesting changes in the materials. It was observed that irradiation caused significant changes in compaction of the glass network. This fact has been supported by IR studies in which the number of non-bridging oxygen's (NBOs) increases.

Alialy *et al.* **[39]** studied the optical properties including infrared and refractive index and density of lithium borate glass as a base glass. The effect of the presence of either aluminum or lead oxide, or the presence of one of the following transition metal, Fe_2O_3, TiO_2 or V_2O_5 was investigated. The effect of exposing the glass to either gamma, or fast neutron irradiation on the last properties was also studied. Glass containing lead oxide had the highest refractive index and density, also the presence of any of the transition metal oxide lowered the average coordination number of oxygen, which causes a compaction of the structure. Hence, an increase in the values of density and refractive index was observed. Since irradiation of glass caused compaction of B_2O_3 by breaking the bonds between triagonal elements, the average ring size became smaller which lead to an increase in density and refractive index too.

Kumar *et al.* **[40]** synthesized $40SiO_2$–$30BaO$–$20B_2O_3$–$10Al_2O_3$ glasses by melt quenching at 1550^o C. Controlled crystallization was carried out to convert these glasses to corresponding glass ceramics. The effect of intermediate oxides on optical properties was investigated using UV–Visible spectra. The intermediate oxides can act as a modifier or network former depending upon chemical composition glasses constituents and their amount. Usually lower amount 25 mol% act as glass former as reported by **N. Lahl** *et al* **[41].**

In the next chapter the sample preparation and details of characterization techniques are given.

Chapter 3 Methodology and Characterization Techniques

3.1 Sample preparation

Sample with composition of $55SiO_2$-$30B_2O_3$-(x)Li_2O-(15-x)Y_2O_3 were prepared by melt quenching technique. The oxides in appropriate amount were mixed in agate mortar pestle for 1 hour (h) in a acetone media. The sample composition, their labels are given in table 3.1. The mixture was melted in an alumina crucible in an electric furnace at various temperatures. Melt was held at melting temperature for 1h to get it homogenized. It was quenched in graphite mould preheated at 300^{o}C. The as quenched samples were annealed at 300^{o}C for 4 h. The furnace was left to cool naturally. After that samples were ground to get the samples in powder form. These samples were characterized using various techniques. The details of the techniques are given I the next section.

Sample ID	**SiO_2**	**B_2O_3**	**Y_2O_3**	**Li_2O**
YL-0	55	30	15	0
YL-5	55	30	10	5
YL-10	55	30	5	10
YL-15	55	30	0	15

3.2 Characterization Techniques

3.2.1 UV-Visible Spectroscopy

The reflectance and absorption in visible range directly affects the perceived color of chemical involved. This technique is complimentary to fluorescence technique, which deals with transition from excited state to ground state, while absorption measure transition from ground state to excited state. Molecules containing π-electrons or non-bonding electrons can absorb the energy in the form of ultraviolet or visible light to excite these electrons to higher anti-bonding molecular orbital. The more easily excited the electrons the longer the wavelength of light it can absorb. The Beer-Lambert law states that the absorbance of a solution is directly proportional to the concentration of the absorbing species in the solution and the path length.

Thus, for a fixed path length, UV/Vis spectroscopy can be used to determine the concentration of the absorber in a solution. It is necessary to know how quickly the absorbance changes with concentration. The instrument used in ultraviolet-visible spectroscopy is called a UV/Vis spectrophotometer. It measures the intensity of light passing through a sample (I), and compares it to the intensity of light before it passes through the sample (I_0). The ratio I/I_0 is called the transmittance, and is usually expressed as a transmittance percentage (%T). The absorbance, A, is based on the transmittance as follows and given in the equation 1.

$$A = - \log(\%T/100\%) \quad (1)$$

The UV-visible spectrophotometer can also be used to measure reflectance. In this case, the spectrophotometer measures the intensity of light reflected from a sample (I), and compares it to the intensity of light reflected from a reference material (I_0). The ratio I/I_o is called the reflectance, and is usually expressed as a percentage (%R). The basic parts of a spectrophotometer are a light source, a holder for the sample, a diffraction grating in a monochromator or a prism to separate the different wavelengths of light, and a detector. The detector is typically a photomultiplier tube, a photodiode, a photodiode array or a charge-coupled device (CCD). Single photodiode detectors and photomultiplier tubes are used with scanning monochromators, which filter the light so that only light of a single wavelength reaches the detector at one time. The scanning monochromator moves the diffraction grating to "step-through" each wavelength so that its intensity may be measured as a function of wavelength. Fixed monochromators are used with CCDs and photodiode arrays. As both of these devices consist of many detectors grouped into one or two dimensional arrays, they are able to collect light of different wavelengths on different pixels or groups of pixels simultaneously.

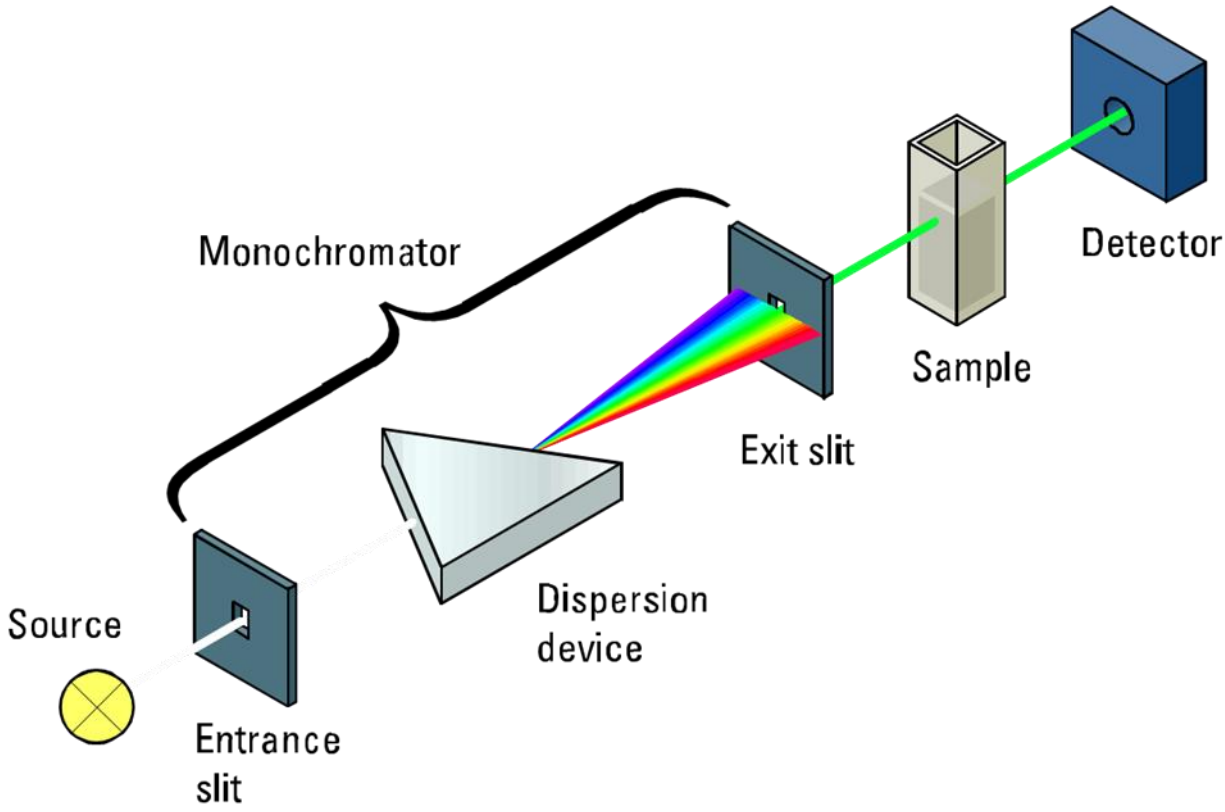

Fig. 3. 1 UV- visible spectrophotometer single beam [42]

In a double-beam instrument, the light is split into two beams before it reaches the sample. One beam is used as the reference; the other beam passes through the sample. The reference beam intensity is taken as 100% Transmission or zero Absorbance, and the measurement displayed is the ratio of the two beam intensities. Some double-beam instruments have two detectors (photodiodes), and the sample and reference beam are measured at the same time. In other instruments, two beams pass through a beam chopper, which blocks one beam at a time. The detector alternates between measuring the sample beam and the reference beam in synchronism with the chopper. There may also be one or more dark intervals in the chopper cycle. In this case, the measured beam intensities may be corrected by subtracting the intensity measured in the dark interval before the ratio is taken.

The samples were ground in agate mortar to obtain these samples in powder form. Diffused reflectance spectrum (DRS) of powder samples was recorded on wavelength range of 240-800

nm using Hitachi 330. Optical band gap and Urbach energy of all the samples were calculated using Kubelka-Munk function [43]

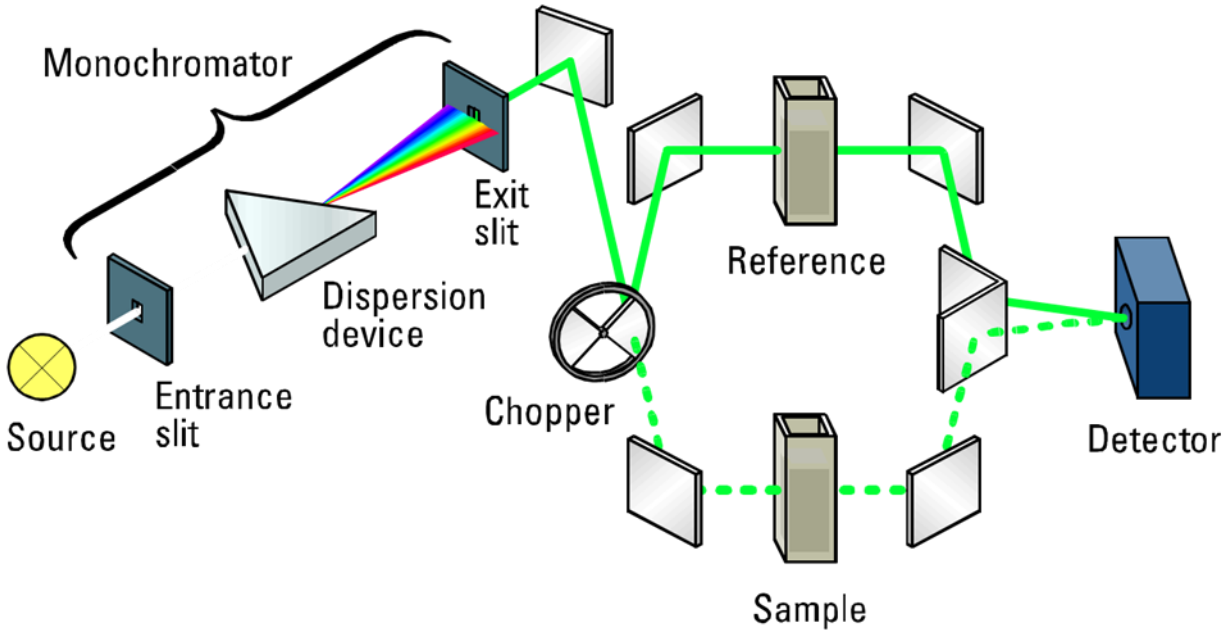

Fig. 3. 2 UV- visible spectrophotometer double beam [42]

Information from UV-Visible Spectroscopy: Using U.V. Visible spectra we can obtain directly or indirectly following information related to various type of samples.

- Direct and indirect optical band gap
- Optical spectrum
- Urbach energy
- Refractive Index etc.

3.2.2 X-ray Diffraction (XRD)

X-ray is a method used for determining the atomic and molecular structure of a crystal, in which the crystalline atoms cause a beam of X-rays to diffract into many specific directions. By measuring the angles and intensities of these diffracted beams, a three-dimensional picture of the density of electrons within the crystal can be produced. From this electron density, the mean positions of the atoms in the

crystal as well as their chemical bonds, their disorder etc. can be determined. X-rays are the form of electromagnetic radiation that have high energy and short wavelength. This wavelength is of the order of atomic spacing within the crystal. When these rays are incident on the material, they get diffracted from the crystal plane as shown in fig 3.3. The reflected rays can interfere both ways destructively as well as constructively. When Bragg's condition is followed, then the reflected rays interfere constructively. The Bragg's equation is given in equation (2):

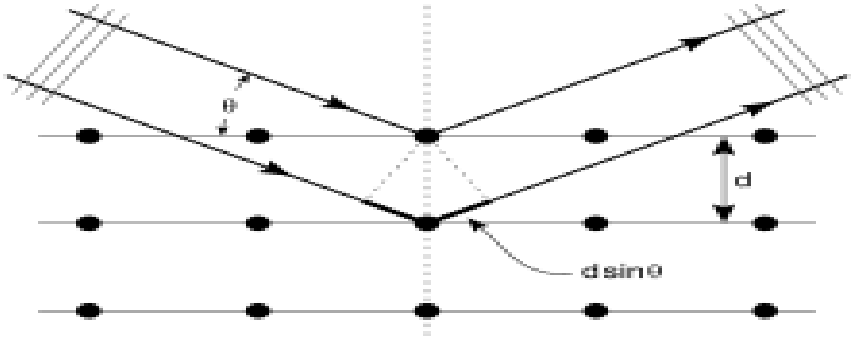

Fig. 3. 3 Diffraction of X-ray by planes of atom [44]

$$2d\sin\theta = n\lambda \quad (2)$$

Where *d* is the inter-planner spacing, θ is the incident angle, *n* is any integer, and λ is the wavelength of the incident beam depending upon target materials. These specific directions appear as spots on the diffraction pattern called reflections. Thus, X-ray diffraction results from an electromagnetic wave impinging on a regular array of scatterers.

- Amorphous nature
- Phase definition and their volume fraction
- Crystallite size
- Lattice parameter
- Strain

The present studied samples were analyzed by PAN analytical X'Pert PRO X-ray diffractometer using λ = 1.54 Å. X-ray diffraction technique was used to check for possible crystallanity of the sample after quenching and annealing. The pattern was recorded at a scanning rate of 6^o min^{-1} between 20-80^o and step size was 0.0130^o.

3.2.3 Fourier Transform Infra Red Spectroscopy (FT-IR):

The main goal of IR spectroscopic analysis is to determine the chemical functional groups in the sample. Different functional groups absorb characteristic frequencies of IR radiation. Using various sampling accessories, IR spectrometers can accept a wide range of sample types such as gases, liquids, and solids.

Infrared radiations having wavenumber from roughly 13,000 to 10 cm^{-1} or wavelength from 0.78 to 1000 μm. Infrared spectroscopy exploits the fact that molecules absorb specific frequencies that are characteristic of their structure. These absorptions are resonant frequencies, i.e. the frequency of the absorbed radiation matches the transition energy of the bond or group that vibrates. A molecule can vibrate in many ways, and each way is called a vibrational mode. For molecules with N atoms in them, linear molecules have 3N – 5 degrees of vibrational modes, whereas nonlinear molecules have 3N – 6 degrees of vibrational modes (also called vibrational degrees of freedom). As an example H_2O, a non-linear molecule, will have $3 \times 3 - 6 = 3$ degrees of vibrational freedom, or modes. Simple diatomic molecules have only one bond and only one vibrational band. If the molecule is symmetrical, e.g. N_2, the band is not observed in the IR spectrum, but only in the Raman spectrum. Asymmetrical diatomic molecules, e.g. CO, absorb in the IR spectrum. More complex molecules have many bonds, and their vibrational spectra are correspondingly more complex, i.e. big molecules have many peaks in their IR spectra. The atoms in a CH_2X_2 group, commonly found in organic compounds and where X can represent any other atom, can vibrate in nine different ways. Six of these involve only the CH_2 portion: symmetric and anti-symmetric stretching, scissoring, rocking, wagging and twisting, as shown below. (Note: because CH_2 is attached to X_2 it has 6 modes as shown in figure 3.4. Unlike H_2O, which only has 3 modes. The rocking, wagging, and twisting modes do not exist for H_2O, since they are rigid body translations and no relative displacements exist.)

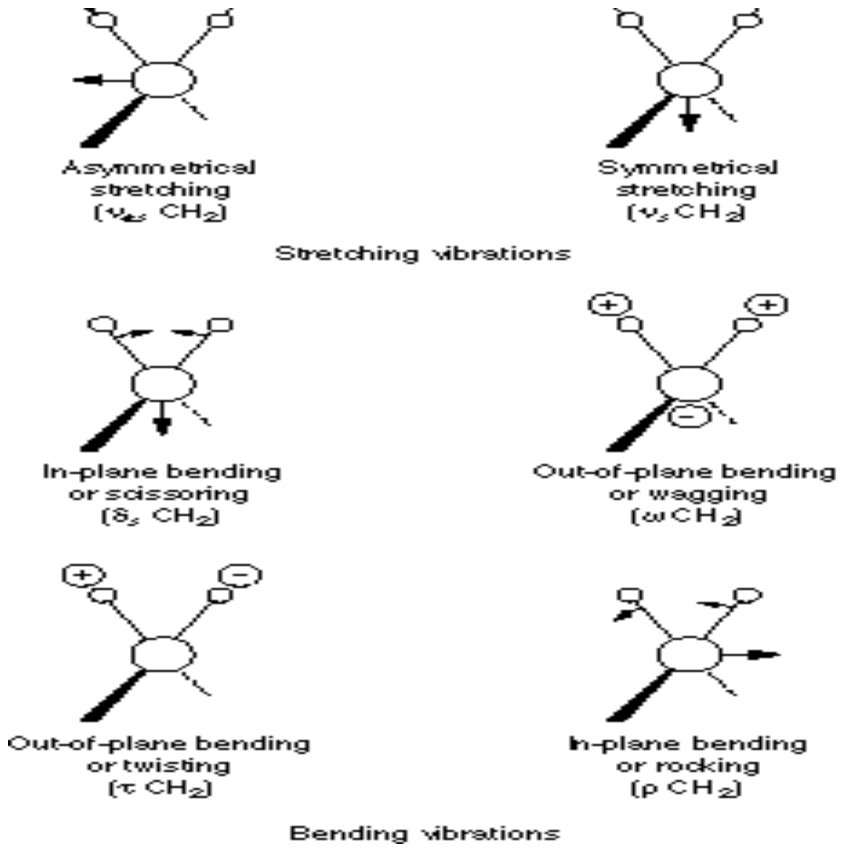

Fig. 3. 4 Number of Vibrational modes of bonds in FTIR [45]

Mechanism of FTIR:

FTIR basically based on principle of Michelson interferometer. It consists of three active components: a moving mirror, a fixed mirror, and a beamsplitter. The two mirrors are perpendicular to each other. The beamsplitter is a semireflecting device and is often made by depositing a thin film of germanium onto a flat KBr substrate. Radiation from the broadband IR source is collimated and directed into the interferometer, and impinges on the beamsplitter. At the beamsplitter, half the IR beam is transmitted to the fixed mirror and the remaining half is reflected to the moving mirror. After the divided beams are reflected from the two mirrors, they are recombined at the beamsplitter. Due to changes in the relative position of the moving mirror to the fixed mirror, an interference pattern is generated. The resulting beam then passes through the sample and is eventually focused on the detector.

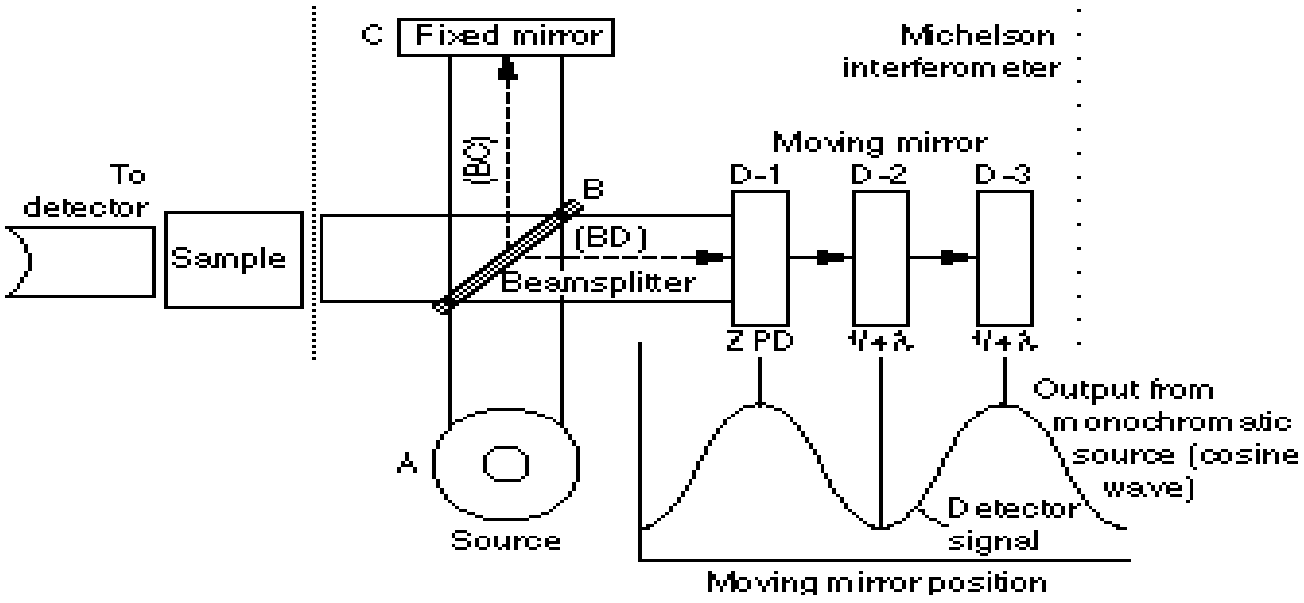

Fig. 3. 5 Simplified optical layout of a typical FTIR spectrometer [45]

The following information about the specimen can be directly extracted from FTIR spectra:

- Bond strength
- Transmittance
- Functional group

3.2.4 Scanning Electron Microscopy (SEM) with EDS:

A scanning electron microscope (SEM) is a type of electron microscope that produces images of a sample by scanning it with a focused beam of electrons. The electrons interact with atoms in the sample, producing various signals that can be detected and that contain information about the sample's surface topography and composition. The electron beam is generally scanned in a scan raster pattern, and the beam's position is combined with the detected signal to produce an image. The most common mode of detection is by secondary electrons emitted by atoms excited by the electron beam. By scanning the sample and detecting the secondary electrons, an image displaying the tilt of the surface is created.

The types of signals produced by a SEM include secondary electrons (SE), back-scattered electrons (BSE), characteristic X-rays, light (cathodoluminescence) (CL), specimen current and transmitted electrons. Secondary electron detectors are standard equipment in all SEMs, but it is rare that a single machine would have detectors for all possible signals. The signals result from interactions of the electron beam with atoms at or near the surface of the sample. In the most common or standard detection mode, secondary electron imaging or SEI, the SEM can produce very high-resolution images of a sample surface, revealing details less than 1 nm in size. Due to the very narrow electron beam, SEM micrographs have a large depth of field yielding a characteristic three-dimensional appearance useful for understanding the surface structure of a sample. Back-scattered electrons (BSE) are beam electrons that are reflected from the sample by elastic scattering. BSE are often used in analytical SEM along with the spectra made from the characteristic X-rays, because the intensity of the BSE signal is strongly related to the atomic number (Z) of the specimen. BSE images can provide information about the distribution of different elements in the sample. The following information can be achieved about ceramic materials.

- Surface topography.
- Elemental information.

3.2.5 Impedance spectroscopy:

Every material has a unique set of electrical characteristics that are dependent on its dielectric properties. A dielectric material measurement provide the information about the loss of cable application, the impedance of substrate, the frequency of dielectric resonator can be related to dielectric properties. This information is also useful for improving ferrite, absorber, and packaging design. Microwave processing of food, rubber, plastic and ceramic have been found from the knowledge of dielectric properties. Agilent measurements measure such as network analyzer, LCR meter, and impedance analyzer range in the frequency of 325 GHz. The present samples are characterized by the impedance analyzer Solartron (SI 1260) at valuable temperature and frequencies. The obtained data are fitted using software Z. view. All the experiments are performed in air using two probe setup.

4.1 X-Ray Diffraction Technique

The amorphous nature of the samples was studied by X-ray diffraction. X ray diffraction pattern of all samples are shown in fig. 4.1. The big broad halos is observed in all samples. In addition to broad halos, the YL-0 exhibit on sharp peak 2θ 27^{o}. The absence of any sharp crystalline peak in YL-5, YL-10, YL-15 indicates that these samples are amorphous in nature.

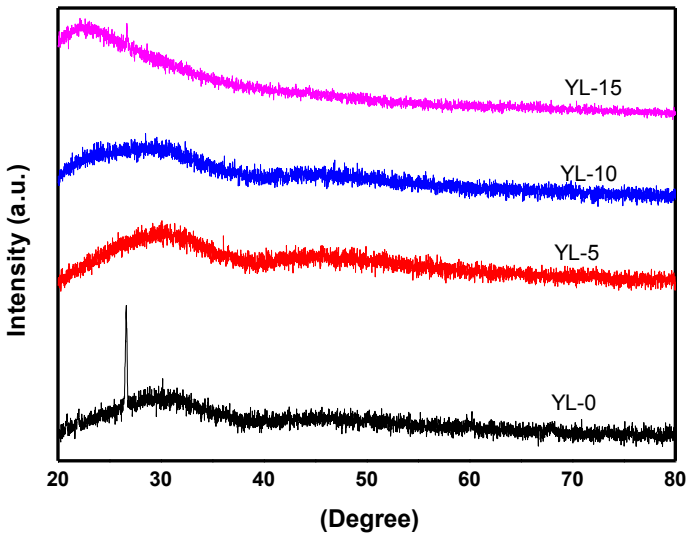

Fig. 4. 1 X-ray diffraction pattern of the samples

The peak is indexed with crystalline phase of SiO_2 (ICDD No.-03-065-0466). Interestingly, the higher the content of intermediate oxide i.e. Y_2O_3 leads to form the crystalline phase i.e. SiO_2. Similarly on the cost of intermediate oxides as the nucleation of the amount of Li_2O increased, in that case SiO_2 crystalline phase also started. Therefore, it is concluded that the higher amount of intermediate oxide or modifier lead to form the crystalline phase. Secondly the higher amount of Y_2O_3 modified the glass matrix more strongly than Li_2O contained glass. Manzo et al. [45] also reported that the higher amount of Y_2O_3 usually lead to increase the thermal stability of glass

4.2 UV-Visible Spectroscopy

To obtain DRS of samples, the ratio of light scattered from thick layer of sample and a ideal non-absorbing reference sample is measured as the function of wavelength λ, $R_\infty = R_{sample}/R_{refernce}$ [46]. The diffused reflectance curves of YL-15 and YL-0 is given in figure 4.2 The relation between DR of the sample (R_∞), absorption coefficient (K) and scattering coefficient (S) is given by the Kubelka-Munk function.

$$F(R_\infty) = (1 - R_\infty^2)/2R_\infty = K/S. \quad (4.1)$$

The optical band gap (E_g) and the linear absorption coefficient (α) of a material are related according to the known Tauc relation as given below:

$$\alpha h\upsilon = A(h\upsilon - E_g)^{n/2} \quad (4.2)$$

where υ is photon energy and A is proportionality constant. When a material scatter in perfectly diffuse manner (or when it is illuminated at 60^o incidence), the K-M absorption coefficient K become equal to 2α. Considering the scattering coefficient S as constant with respect to wavelength and using Eqs. (1) and (2) the following expression can be written as:

$$F(R_\infty)h\upsilon = B(h\upsilon - E_g)^n. \quad (4.3)$$

Where, B is proportionality constant. For a semiconductor samples $(F(R)\ h\nu)^{1/n}$ vs $h\nu$. For a direct band gap semiconductor the plot $n = 1/2$ will show a linear just above the optical absorption edge. This linear portion can be extrapolated and made to cut the x-axis corresponding to $(F(R)h\nu)^2 = 0$. The intercept gives the value of direct optical band gap. Indirect band gap materials on the $n = 2$ plot [47].

In present case, $(F(R)\ h\nu)^2$ was plotted against the photon energy $h\nu$ as shown in figure 4.3 . It is observed that with the increase of Y_2O_3 there is decrease in optical band gap. As discussed in the section of X-rays diffraction Y_2O_3 act as glass modifier in the present studied samples. Therefore it can be concluded that Y^{3+} has much tendency to break the network formed by B_2O_3 with non-bridging oxygen (NBOs). Large number of NBOs is created on breakage of network. Absorption of light energy in glasses and glass ceramic is mainly due to loosely

bounded of these NBO's. The creation of NBO's enhance the possibility of electronic transition and lower the band gap. Although Li_2O is also a network modifier, however in the present case Y_2O_3 seems to modify the glass network to greater extent than that of Li_2O.

The main feature of the absorption edge of amorphous materials is an exponential increase of the absorption coefficient with photon energy. When the energy of the incident photon is less than the band gap, the increase in absorption coefficient is followed with an exponential decay of density of states localized into the optical band gap [48]. The lack of crystalline long-range ordering glassy material sis associated with at tailing of density of states into forbidden energy [44]. The band tail associated with valence band and conduction band, which is developed due to the potential fluctuations in the material, extends into the energy gap and normally shows an exponential behavior. Urbach energy characterizes the extent of the exponential tail of the absorption edge is characterized by a parameter called Urbach energy [49]. Absorption coefficients in Urbach tail region vary in accordance with following relation:

$$\alpha = \alpha_o \exp(h\nu / E_u) \qquad (4.4)$$

Here α_o is a constant; E_u is the Urbach energy can calculated from ln F(R) vs photon energy plot, by taking reciprocal of the slopes of linear portion. Generally, the Urbach energy depends on the defects in the materials. Value of Urbach energy increased with Y_2O_3 amount, which again is the manifestation of presence of more defect with Y_2O_3 addition. On the other hand YL-10 and YL-15 samples have minimum Urbach energy, indicating relatively less defects.

Table 4.1 Optical parameters, namely, band gap (eV) and Urbach energy of YL-0, YL-5, YL-10 and YL-15 samples.

Sample ID	Band gap (eV)	Urbach energy (eV)
YL-0	3.64	0.51
YL-5	3.71	0.45
YL-10	3.81	0.33
YL-15	3.90	0.31

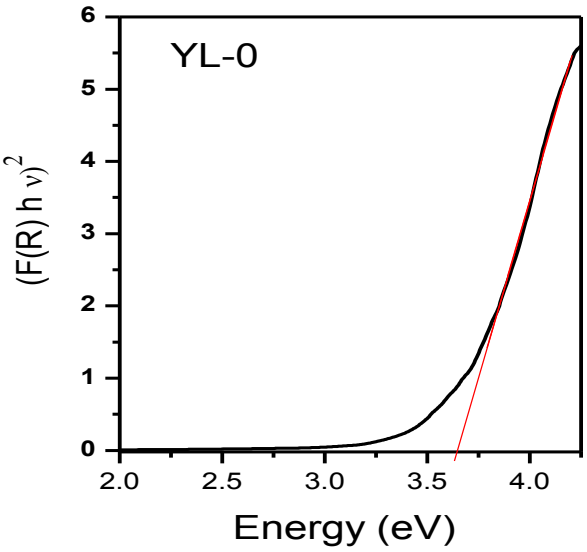

(a)

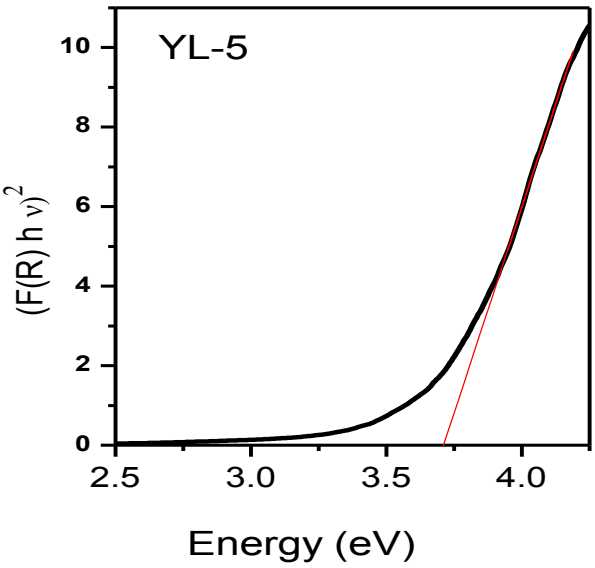

(b)

Fig. 4. 2 Band gap of (a) YL-0 (b) YL-5

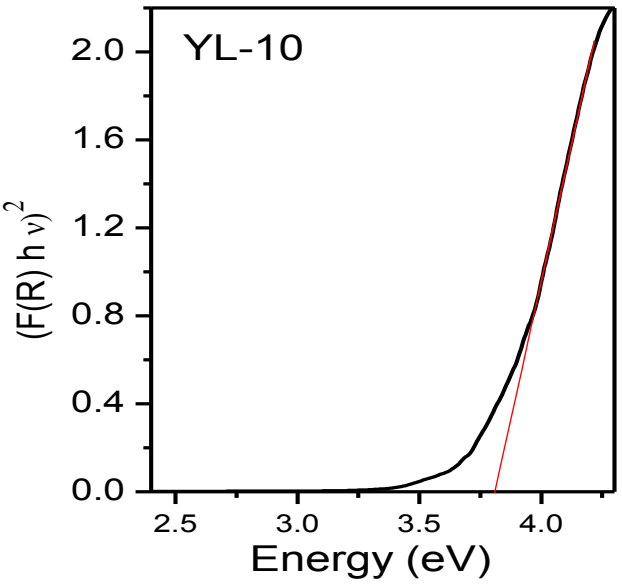

(c)

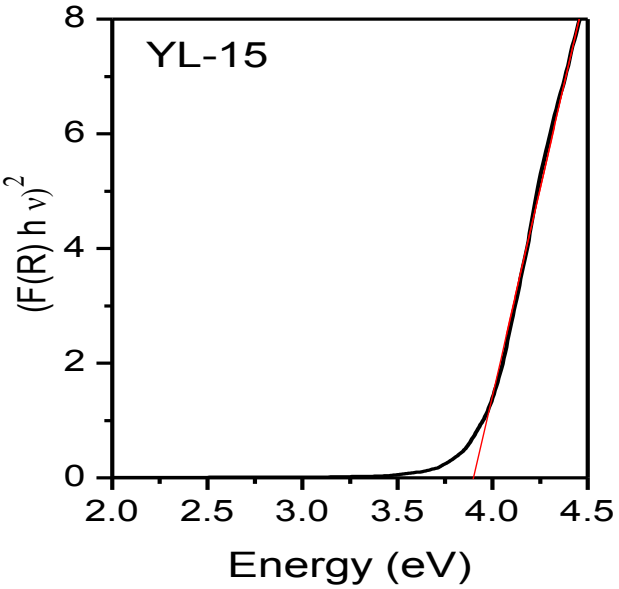

(d)

Fig. 4. 3 Band gap of (c) YL-10 (d) YL-15

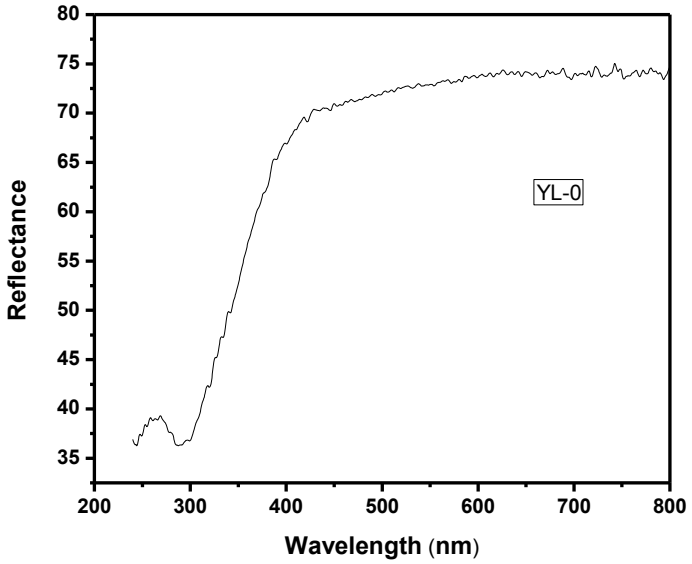

(a)

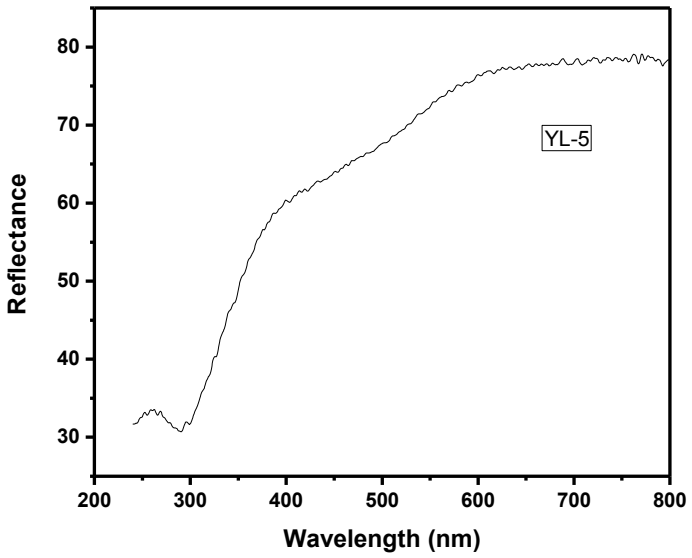

(b)

Fig. 4.3 Reflection Spectra of (a)YL-0 (b) YL-5.

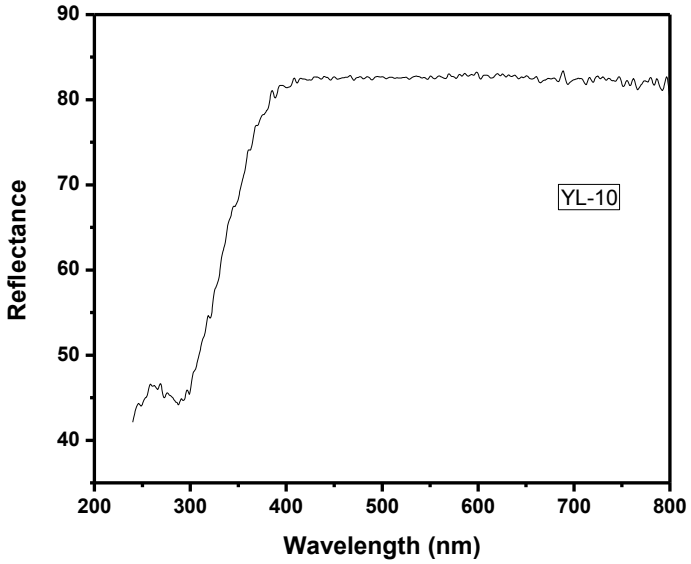

(c)

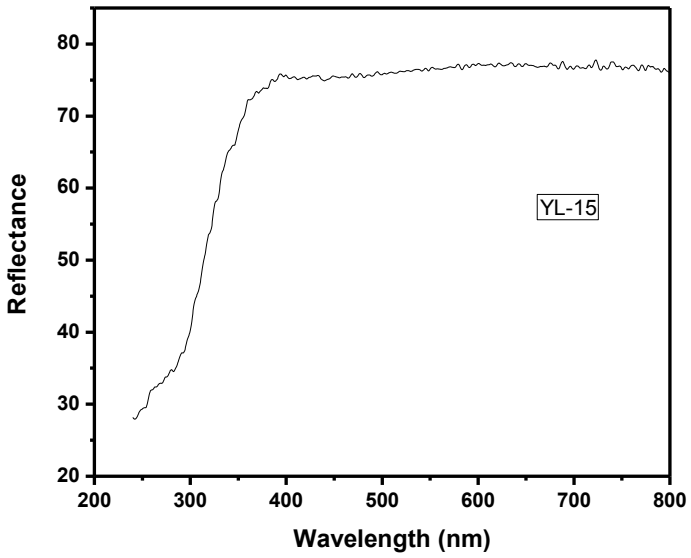

(d)

Fig. 4.3 Reflection Spectra of (c) YL-10 (d) YL-15 samples.

4.3 FTIR Analysis

Samples shows major transmittance bands at around 680 cm^{-1}, 1080 cm^{-1}, 1375 cm^{-1}, 2350 cm^{-1} with some minor changes in band intensities and peak positions with respect to each other. The most intense and broad band is observed at around 1080 cm^{-1}. It can be attributed to the combined stretching vibration of Si-O-Si and B-O-B network of tetrahedral structural units. The band at 1335 cm^{-1} are due to B-O stretching of bonds. The bands extending from nearly 2200-4000 cm^{-1} are due to OH and B-OH vibrations including the characteristic near infrared absorption bands of water [50]. The FTIR band at 680 cm^{-1} may attribute due to combined vibration of AlO_6 & vibration of bridging oxygen between trigonol boron atoms [51]. Band width in FTIR spectra is due to the homogeneity of chemical bonding. As in most intense and broad peak at 1080 cm^{-1} shows maximum sharpness for YL-0 samples. It is good agreement with XRD results, where this is showing crystalline phase of SiO_2. The bond length and bond angles are well defined. As the broadening of transmittance band appears due to heterogeneous distribution of bonds parameter, the sharpness of this particular band is attributed to the crystalline phase present in glass network. This means due to increase in lithium oxide causes defect due to which strain in chemical bonding which changes the bond strength. The peak at 1375 cm^{-1} is shifted to higher wave number with increase of lithium oxide. In addition to this, reduction in Li^{2+} changes the coordination number with higher NBOs. The presence of metal cation in silica network induces transformation of SiO^- group. The non appearance of sharp bands can be attributes to the possible tendency of the structure to more randomness or amorphicity of the structure. This fact is supported by the increase in the values of Urbach Energy after irradiating the sample. This could also be assigned to changes in the bond angles or bond lengths of the building units that is, Si–O–Si and B–O–B [52].

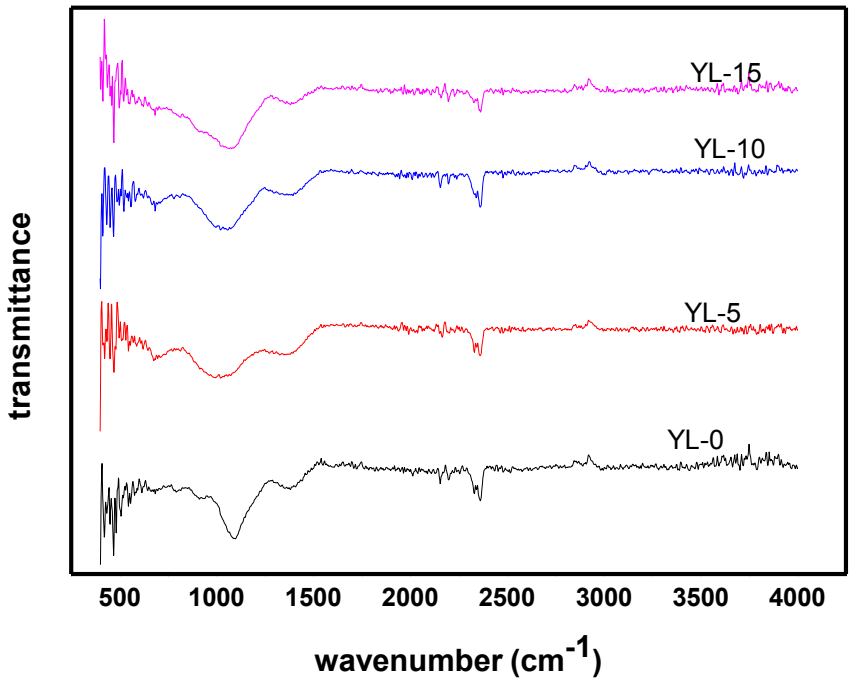

Fig. 4.4 FTIR Spectra of YL-0, YL-5, YL-10, YL-15

4.4 Dielectric Properties

Lithium borates are classical glass forming systems, which have been extensively studied in the literature. Li has high sensitivity with respect to scattered neutrons because the resonance peak energy of the Li reaction cross-section corresponds to the back scattered neutron energy and due to this fact materials containing Li are considered as ideal scintillators for detection of scattered neutrons in nuclear fusion [52]. Lithium borate glasses doped with rare earths such as Ce, Eu, Tb, Sm and Yb have been studied for scintillating applications [53-55]. Glasses doped with rare earth ions have been investigated intensively for photonics, optoelectronics and scintillating applications [56-58]. Electrical conductivity of binary Li_2O-B_2O_3 glasses has been studied and the conductivity was found to be ionic nature due to small size of the ion, low mass and large electropositivity [59].

The effect of the temperature on the conductivity of Y_2O_3 containing glasses and other parameters is given in Table 4.2. It is observed that conductivity of all glass samples increases with increase in temperature. The equivalent circuit for low-temperature region represents three parts in series: R1 resistance, and two Voight elements (R and CPE in parallel). R1 stands

for volume resistance of the sample, CPE1 is a constant phase element that corresponds to charge transfer. Capacities values for elements describing corresponding semicircles are typical for volume conductivity component (10^{-11}–10^{-12} F) and grain boundary component (10^{-9}–10^{-10} F). R1 resistance stands for intragranular (volume) conductivity, parallel connection CPE1 – for transfer through grain boundaries. Thus general conductivity is a sum of intragranular and grain boundaries conductivity. This value was used to determine conductivity of a polycrystalline sample. In this case general conductivity is defined by R1 resistance only (comprising both bulk and grain boundary resistances).

Table 4.2 Resistance, capacitance and conductivity of YL-5 samples.

Temp (K)	**Resistance (ohm)**	**Capacitance (farad)**	**Conductivity (simen/m)**
360	$2.16*10^{7}$	$3.35*10^{-11}$	$7.92*10^{-10}$
430	$1.79*10^{6}$	$2.59*10^{-11}$	$9.61*10^{-9}$
440	$1.29*10^{6}$	$2.59*10^{-11}$	$1.33*10^{-8}$
450	$9.90*10^{5}$	$2.74*10^{-11}$	$1.73*10^{-8}$
460	$7.62*10^{5}$	$2.53*10^{-11}$	$2.25*10^{-8}$
500	$3.06*10^{5}$	$2.54*10^{-11}$	$5.61*10^{-8}$

The Cole-Cole plot of YL-5 at two different temperature are given in fig 4.5 (a) and 4.5 (b). The semi circle is fully resolved in the present sample. The conductivity $5.61*10^{-6}$ s/cm at 500^{o}C.

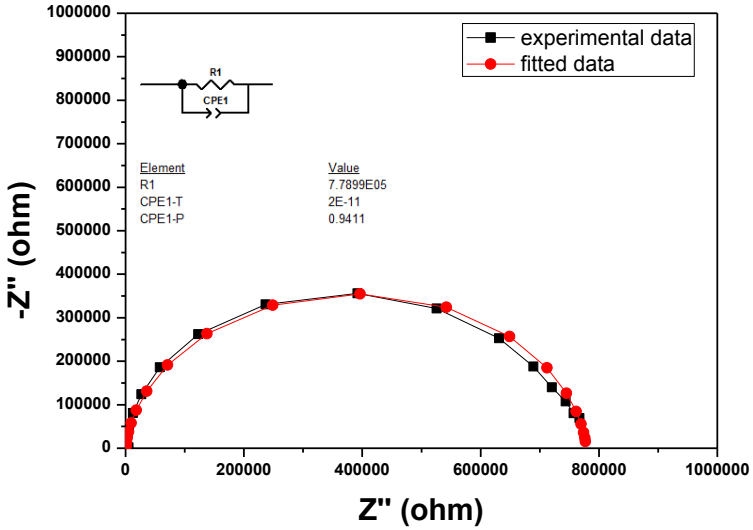

(a) Cole-cole Plot of YL-5 at 459^{o}C

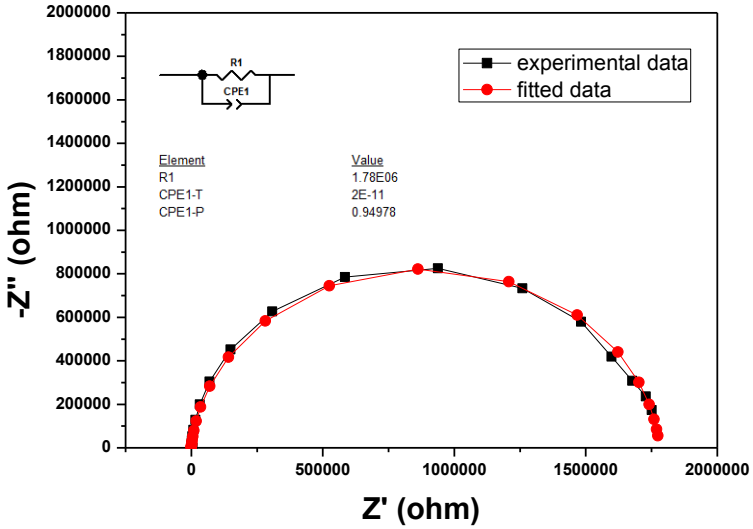

Fig. 4.5 Cole-cole Plot of YL-5

4.5 SEM Analysis

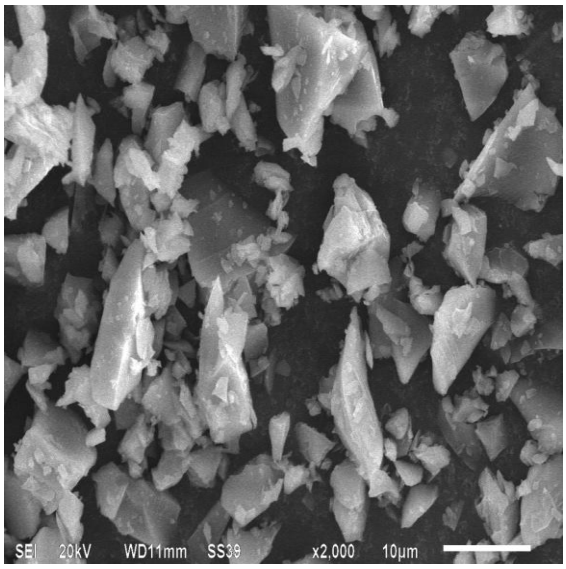

Fig. 4.6 (a) SEM of YL-5

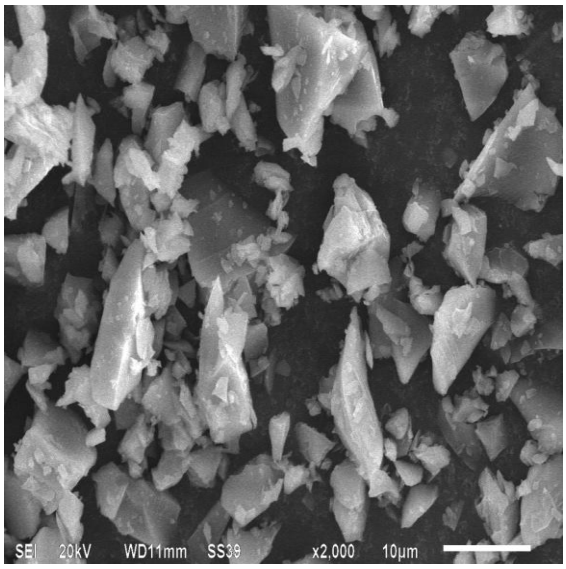

Fig. 4.6 (b) SEM of YL-10

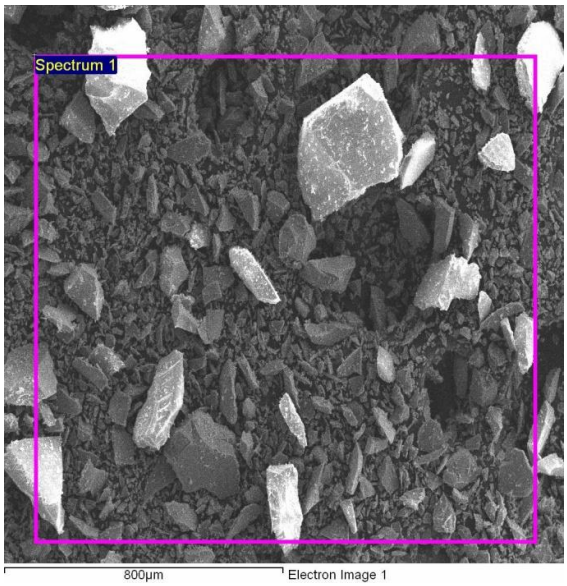

Fig. 4.7 (a) SEM of YL-5

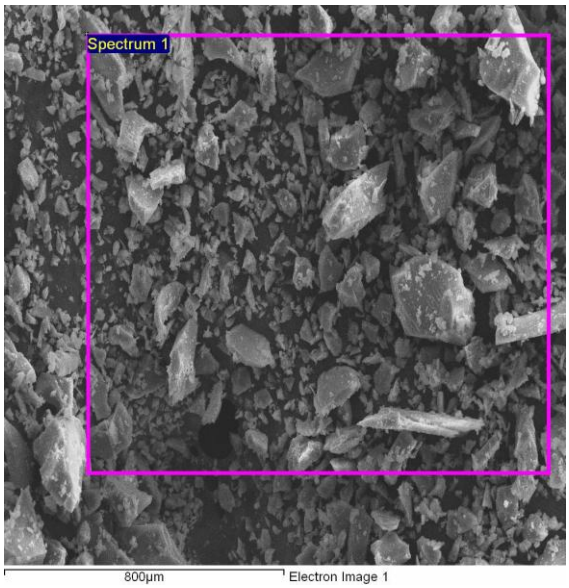

Fig. 4.7 (b) SEM of YL-10

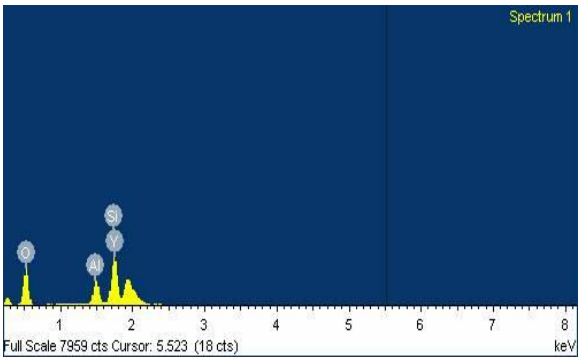

Fig. 4.8 (a) EDS of YL-5

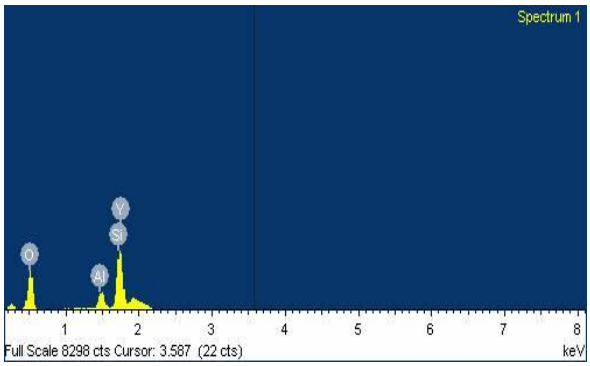

Fig. 4.8 (b) SEM of YL-10

Fig. 4.6 (a) and fig. 4.6 (b) show the SEM micrographs of the samples YL5 and YL10. Before SEM measurements powder form of samples had been gold sputtered. Both micrographs have been taken on the same magnifications. Both micrographs clearly indicate that it has more or less same microstructural features. It is also observed from micrographs no secondary phase is formed in the prepared samples. The faceted morphology in both micrographs clearly indicates the role of SiO_2 in the glass formation. SiO_2 based glasses, generally have faceted type of morphology. Moreover, for elemental analysis EDS is also done on a selected area. Fig 4.8 (a) and fig. 4.8 (b) shows the area of sample analyzed by EDS. It shows the presence of Si, O, Y and Al element which are also presented in table 4.3. In our initial composition we had not been taken the Al based compounds. Here in our case we melted our samples in the alumina (Al_2O_3) crucible. It might be possible that during melting some part of Al_2O_3 got reacted with the glasses and it is observed in EDS.

Table 4.3 Presence of Si, O, Y and Al element in YL-5 sample

Element	Weight (%)	Atomic (%)
O	54.44	76.10
Al	7.14	5.91
Si	15.28	12.16
Y	23.15	5.82

Table 4.3 Presence of Si, O, Y and Al element in YL-10 sample

Element	Weight (%)	Atomic (%)
O	59.67	75
Al	5.85	4.41
Si	23.84	17.27
Y	10.64	2.44

4.6 Conclusion

The four glasses were synthesized by melt-quenched technique. The higher content of intermediate oxides/modifier leads to prevent the glass formation. Crystalline SiO_2 phase is formed in YL-0 and YL-15 samples. The optical band gap increase with increasing Y_2O_3 content in glasses. However Urbach energy could not follow any tread. The total conductivity is observed in the insulating range ~$5.91*10^{-6}$ s/cm at 600^0C for YL-5 glass.

4.7 Future Scope

The present glasses should be characterized by DTA/TGA. To know their glass transition temperature crystallization temperature and melting temperature of the glasses so that the thermal stability of glasses could be find out.

The present glasses comprehensive exhibit Li_2O as a constituent, so these glasses may be used as solid electrolyte for battery application. For this the conductivity of all the glasses should be measured upto 800^oC in oxidizing atmosphere.

References

1 F. Subiaul, F. Jessica. C. Ralph, L. Holloway and H. S. Terrace,*J. mater. Sci*., **305** (2004) 407.

2 W. M. Allen, B. F. Sansom, C. F. Drake and D. C. Davies,*J. Ceram. Engg. & Sci. Proceed*, **2** (1978) 73.

3 W. M. Allen, B. F. Sansom, P.T. Gleed, C.B. Mallinson and C.F. Drake, *J.American Ceramic Society,* **55** (1984) 115.

4 Ravenscroft, Edward, 2nd Edition **53** (1707) 152.

5 J.E. Shelby, 2nd Edition, RS.C, **48** (1994) 225.

6 J. Fraunhofer*optical institute Benediktbeuren* **58** (1787) 239.

7 Department of glass and technology in *Shiffield University Germany* (1915).

8 Agricola, Georgius, De re metallica, translated by Herbert Clark Hoover and Lou Henry Hoover and Dover De Re Metallica, *Trans. by Hoover Online Version,* **76** (2007) 567.

9 H. Wilde, TechnologischeInnovationen, JahrtausendZur, Verwendung und Verbreitungneuer, WerkstoffeostmediterranenRaum and Patrick McCray,*J. Amer. Ceram. Soc.*,**44** (2003) 25.

10 Bayley, In Price, **67** (2000) 176.

11 D.E. Day, J. E. White, R. F. Brown and K. D. Mcmenamin, J.*Glass Tech.*, **44** (2003) 75.

12 S.A. Aly, S. A. Mahmoud, N. Z. El – Sayed and M.A. Kaid, *J. of phy. and chem. of solids*, **55** (1999) 159.

13 M. N. Rahman, W. Liang, D. E. Day, N. W. Morion, G. C. Reilly and J. Mao, *J. Ceram. Engg. & Sci. Proceed*, **56** (2005) 26.

14 M. Magallane, Perdomoa, A. H. De. Aza, I. Sobrados, J. Sanz and P. Pena,*J.Acta Biomaterial,* **8** (2012) 820

15 A. Dutta and A. Ghosh, *J. Non-Cryst. Solids*, **353** (2007) 1333.

16 F. Borsa, D.R. Torgeson, S.W. Martin and H.K. Patel, *Phys. Rev. B*,**46** (1992) 795.

17 Y. Dimitriev, V. Mihailova and E. Gattef, *Phys. Chem. Glasses*, **34** (1986) 14.

18 D.W. Hall, M.A. Newhouse, N.F. Borrelli, W.H. Dumbaugh and D.L. Weidman, *Appl. Phys. Lett.* **54** (1989) 1293.

19 S. Hazra, S. Mandal and A. Ghosh, *Phys. Rev*. B **56** (1997) 8021.

20 L. Baia, R. Stefan, W. Kiefer, J. Popp and S. Simon, *J. Non-Cryst. Solids* **303** (2002) 379.

21 J. Yang, S. Dai, N. Dai, S. Xu, L. Wen, L. Hu and Z. Jiang, *J. Opt. Soc. Am. B* **20** (2003) 810.

22 W.H. Dumbaugh and J.C. Lapp, *J. Am. Ceram. Soc.***75** (1992) 2315.

23 E.M. Vogel, M.J. Weber and D.M. Krol, *Phys. Chem. Glasses* **32** (1991) 231.

25 K. D. Mcmenamin, S. A. Mahmoud, Patrick McCray, D. E. Day and N. W. Morion, *J. Ceram.Engg. & Sci* .**86** (2010) 125.

26 Graham, *Phil. Trans. of the Roy. Soc.*, **243** (1833) 123.

27 J. H. Campbell and T. I. Suratwala, *Univ. conf. on glass sci*., **26** (2000) 263.

28 S.A. Aly, S. A. Mahmoud, N. Z. El – Sayed and M.A. Kaid, *Phil. Trans. of the Roy. Soc* **55** (1999) 159.

29 R. S. Gedam and D. D. Ramteke, *J. of phy. and chem. of sol*. **74** (2013) 1399-1402.

30 N. Ahlawat, S. Sanghi, A. Agarwal and R. Bala, *Journal of mol. Struc.* **963** (2010) 82-86.

31 R. S. Gedam and D.D. Ramteke, *Rare earths* **8** (2012) 785.

32 N. Gupta, K. Singh and O.P. Pandey, *J Mater Sci* **42** (2007) 6426.

33 Y. Liu, J. Huang, X. Wang, Q. Yang, Y. Wang, P. Rao and Q. Wang, *New J. of Glass and ceram.***1** (2011) 53.

34 Sae- Fue Wang, Yung-Fu Hsu, Chieh-sheng Cheng andYueh- Chi Hsieh, *International J. of hydrozen energy* **38** (2013) 14779.

35 Y. H. Kim, M. Y. Yoon, E. J. Lee and H. *J.* Hwang, *J. of Ceram. Proc. Res.***13** (2012) 37.

36 T. Dalvi, H. Monma and K. Yamashita, *J. of the Euro. Ceram. So.***26**(2006) 619.

37 J.E. Garbarczyk, M. Wasiucionek, P. Jozwiak, J.L. Nowinski and C. M. Julien, *Solid state Ionics* **180** (2009) 531.

38 R. Kaur, S. Singh, K. Singh and O.P. Pandey *Rad. Phy.and Chem.***86** (2013) 23.

39 N.A. El-Alaily and R.M. Mohamed *Mater. Sci. and Engg.***98** (2003) 193.

40 V. Kumar,O.P.Pandey andK.Singh,*Physica B***405** (2010) 204.

41 L. Lahl and H. A. El-Batal. *J. Pure Appl. Phys*. **35** (1997) 579.

42 N. Gupta and A.Dalvi*Solid State Ionics***225** (2012) 363.

43 P. Mishra and M. A. Dubinskii, "Ultraspectroscopy and UV laser " *New York marcel dekker* (2002)

44 http://serc.carleton.edu/research_education/geochemsheets/BraggsLaw.html.

45 http://en.wikipedia.org/wiki/FourierTransformInfraredRadiation.

46 S. Cruz-Manzo and R. Chen,*J. of Electro. Chem.*,**694** (2013) 45.

47 R. Nelson, M. H. Weatherspoon, J. Gomez, E.E. Kalu and J. P. Zheng, *Electrochem. Comm.***34** (2013) 77.

48 F. A. Khalifa and H. A. El-Batal.*J. Pure Appl. Phys*. **35** (1997) 579.

49 G. Sharma, K. Singh, Manupriya, S. Mohan, H. Singh and S. Bindra, *J. Radiat.Phys.Chem.***75** (2006) 959.

50 F. Urbach, *Phys. Rev*. **92** (1953) 1324.

51 Y. Takahashi and K. Yamaguchi, *J. Mater. Sci*. **25** (1990) 3950.

52 M. Tatsumisago, K. Yoneda, N. Machida and T. Hinami,*J. Non-Cryst.Solids* **95** (1987) 857.

53 B.P.Dwivedi, M.H. Rahman, Y. Kumar and B.N. Khanna, *J. Phys .Chem. Solids* **54** (1993) 621.

54 F.E. Salman, N. Shash, H. Abou El-Haded and M.K. El-Mansy, *J. Phys. Chem .Solids* **63** (2002) 1957.

55 H. Wada, M. Menetrier, A. Levasseur and P. Hagenmuller, *Mater. Res. Bull*. **18** (1983) 189.

56 C. Lurin, C. Parent, G. LeFlem and P. Hagenmuller,*J. Phys. Chem. Solids* **46** (1985) 1083.

57 S.S.L. Surana, Y.K. Sharma and S.P. Tandon, *Laser Mat. Sci. Eng* .B **83** (2001) 204.

58 M. Prashant Kumar and T. Sankarappa, *J. Non-Cryst. Solids* **355** (2009) 295.

59 W.H. Dumbaugh and J.C. Lapp, *J. Am. Ceram. Soc*. **75** (1992) 2315.

60 Y. Takahashi and K. Yamaguchi, *J. Mater. Sci*. **25** (1990) 3950.